UNIVERSITY OF COPENHAGEN

Second harmonic generation microscopy investigation of the crystalline ultrastructure of three barley starch lines affected by hydration

Cicek, Richard; Tokarz, Danielle; Steup, Martin; Tetlow, Ian J.; Emes, Michael J.; Hebelstrup, Kim H.; Blennow, Andreas; Barzda, Virginijus

Second harmonic generation microscopy investigation of the crystalline ultrastructure of three barley starch lines affected by hydration

Richard Cisek,[1] Danielle Tokarz,[1] Martin Steup,[2,3] Ian J. Tetlow,[3] Michael J. Emes,[3] Kim H. Hebelstrup,[4] Andreas Blennow,[5] and Virginijus Barzda[1,*]

[1]*Department of Chemical and Physical Sciences, Department of Physics and Institute for Optical Sciences, University of Toronto, 3359 Mississauga Road, Mississauga, ON, L5L 1C6, Canada*
[2]*Department of Plant Physiology, Institute of Biochemistry and Biology, University of Potsdam, Karl-Liebknecht-Strasse 24-25 Building 20, 14476 Potsdam, Germany*
[3]*Department of Molecular and Cellular Biology, College of Biological Science, Summerlee Science Complex, University of Guelph, 50 Stone Road East, Guelph, ON, N1G 2W1, Canada*
[4]*Department of Molecular Biology and Genetics, Aarhus University, Forsøgsvej 1, 4200 Slagelse, Denmark*
[5]*Department of Plant and Environmental Sciences, University of Copenhagen, Thorvaldsensvej 40, 1871 Frederiksberg C, Denmark*
*virgis.barzda@utoronto.ca

Abstract: Second harmonic generation (SHG) microscopy is employed to study changes in crystalline organization due to altered gene expression and hydration in barley starch granules. SHG intensity and susceptibility ratio values (R'_{SHG}) are obtained using reduced Stokes-Mueller polarimetric microscopy. The maximum R'_{SHG} values occur at moderate moisture indicating the narrowest orientation distribution of nonlinear dipoles from the cylindrical axis of glucan helices. The maximum SHG intensity occurs at the highest moisture and amylopectin content. These results support the hypothesis that SHG is caused by ordered hydrogen and hydroxyl bond networks which increase with hydration of starch granules.

References and links

1. A. E. Tuer, M. K. Akens, S. Krouglov, D. Sandkuijl, B. C. Wilson, C. M. Whyne, and V. Barzda, "Hierarchical model of fibrillar collagen organization for interpreting the second-order susceptibility tensors in biological tissue," Biophys. J. **103**(10), 2093–2105 (2012).
2. S. W. Chu, S. Y. Chen, G. W. Chern, T. H. Tsai, Y. C. Chen, B. L. Lin, and C. K. Sun, "Studies of χ(2)/χ(3) tensors in submicron-scaled bio-tissues by polarization harmonics optical microscopy," Biophys. J. **86**(6), 3914–3922 (2004).
3. D. Tokarz, R. Cisek, S. Krouglov, L. Kontenis, U. Fekl, and V. Barzda, "Molecular organization of crystalline β-carotene in carrots determined with polarization-dependent second and third harmonic generation microscopy," J. Phys. Chem. B **118**(14), 3814–3822 (2014).
4. S. Psilodimitrakopoulos, I. Amat-Roldan, P. Loza-Alvarez, and D. Artigas, "Effect of molecular organization on the image histograms of polarization SHG microscopy," Biomed. Opt. Express **3**(10), 2681–2693 (2012).
5. A. Buléon, P. Colonna, V. Planchot, and S. Ball, "Starch granules: Structure and biosynthesis," Int. J. Biol. Macromol. **23**(2), 85–112 (1998).
6. J. Blazek and E. P. Gilbert, "Application of small-angle x-ray and neutron scattering techniques to the characterisation of starch structure: A review," Carbohydr. Polym. **85**(2), 281–293 (2011).
7. Z. Y. Zhuo, C. S. Liao, C. H. Huang, J. Y. Yu, Y. Y. Tzeng, W. Lo, C. Y. Dong, H. C. Chui, Y. C. Huang, H. M. Lai, and S. W. Chu, "Second harmonic generation imaging - a new method for unraveling molecular information of starch," J. Struct. Biol. **171**(1), 88–94 (2010).
8. R. Cisek, D. Tokarz, S. Krouglov, M. Steup, M. J. Emes, I. J. Tetlow, and V. Barzda, "Second harmonic generation mediated by aligned water in starch granules," J. Phys. Chem. B **118**(51), 14785–14794 (2014).
9. M. Carciofi, A. Blennow, S. L. Jensen, S. S. Shaik, A. Henriksen, A. Buléon, P. B. Holm, and K. H. Hebelstrup, "Concerted suppression of all starch branching enzyme genes in barley produces amylose-only starch granules," BMC Plant Biol. **12**(223), 223 (2012).

10. R. Carriles, D. N. Schafer, K. E. Sheetz, J. J. Field, R. Cisek, V. Barzda, A. W. Sylvester, and J. A. Squier, "Invited review article: Imaging techniques for harmonic and multiphoton absorption fluorescence microscopy," Rev. Sci. Instrum. **80**(8), 081101 (2009).
11. A. Major, R. Cisek, D. Sandkuijl, and V. Barzda, "Femtosecond Yb:KGd(WO4)2 laser with > 100 nJ of pulse energy," Laser Phys. Lett. **6**(4), 272–274 (2009).
12. M. Samim, S. Krouglov, and V. Barzda, "Double stokes mueller polarimetry of second-harmonic generation in ordered molecular structures," J. Opt. Soc. Am. B **32**(3), 451–461 (2015).
13. A. E. Tuer, S. Krouglov, N. Prent, R. Cisek, D. Sandkuijl, K. Yasufuku, B. C. Wilson, and V. Barzda, "Nonlinear optical properties of type I collagen fibers studied by polarization dependent second harmonic generation microscopy," J. Phys. Chem. B **115**(44), 12759–12769 (2011).
14. T. Y. Bogracheva, Y. L. Wang, and C. L. Hedley, "The effect of water content on the ordered/disordered structures in starches," Biopolymers **58**(3), 247–259 (2001).
15. A. M. Donald, K. L. Kato, P. A. Perry, and T. A. Waigh, "Scattering studies of the internal structure of starch granules," Starke **53**(10), 504–512 (2001).

1. Introduction

Second harmonic generation (SHG) microscopy is an effective analytical tool for structural investigations of ordered, non-centrosymmetric biological samples. Polarization-dependent SHG can deduce nanoscale molecular organization, as shown for collagen [1], muscle [2], β-carotene aggregates [3], and starch granules [4] without pre-treatment with molecular dyes.

Quantitative imaging requires classification and ultrastructural characterization of SHG emitting structures. A starch granule can be considered as a model biological structure for SHG microscopy. It has a radial structure and therefore, SHG polarization images provide visual information about the laser polarization state. Starch granules are mainly composed of just two types of α-glucans, amylose and amylopectin. Amylose is a mixture of unbranched and poorly branched glucans covering a wide range of degree of polymerization, but has a smaller size than amylopectin. Typically, the latter is the quantitatively dominant constituent of the granule possessing approximately 95% α-1,4 interglucose linkages and 5% of branching points, i.e. α-1,6 bonds. In amylopectin, adjacent glucan chains can form double helices since branching points are clustered, giving rise to the semicrystalline amylopectin structure. Amorphous regions are enriched in branching points while crystalline areas are formed by highly ordered double glucan helices, the organization of which leads to the A- or B-type allomorph of the entire starch granules [5]. The nanoscale ultrastructure of starch structures is highly variable and affected by chemical parameters, such as chain length distribution, frequency of branching points as well as physical factors, such as temperature and the degree of hydration [6].

The focus of this study is to determine the ultrastructural organization of crystallites responsible for intense SHG and to understand the organization of the entire starch granule. Previous studies identified two factors affecting SHG in starch granules: i) amylopectin content [7], and ii) hydration conditions [8]. To understand the relation of the two parameters to the ultrastructure of the crystallites, barley reserve starch granules from wild type (WT, cv. Golden Promise) and two transgenic lines were used. Barley WT has an amylose content ~30% of the reserve starch dry weight. One starch line (Waxy, WX; genetic background cv. Cinnamon) lacks granule-bound starch synthase which forms amylose, resulting in starch consisting essentially of amylopectin and, in rice, maize and potato it induces stronger SHG intensity than WT [7, 8]. The other starch line is a so-called amylose only (AO; background Golden Promise) barley line generated by suppression of all genes encoding starch branching enzymes [9], and largely consists of amylose and amylopectin which is modified to generate a loosely branched structure with lower molecular weight. Its branching point frequency, thermal properties and lower apparent molecular weight are similar to amylose. The ultrastructure of the three starch samples will be investigated under different hydration conditions by SHG microscopy.

2. Materials and methods

2.1 Sample preparation

All reserve barley starch granules were studied *in vitro* under 3 conditions: hydrated, air-dried, and ultra-dried. The lines were grown in identical conditions at the field station AU Flakkebjerg/Denmark (55°19′26.7"N 11°23′23.7"E) over the summer of 2013. Grains from the homozygous T_3 generation were used for starch isolation, and were harvested after complete maturation and desiccation [9]. Starch granules were prepared from barley using a mild aqueous method to preserve granule crystallinity. The dry granules were fully hydrated by agitating in 20 mM Tris-HCl (pH 7.5) for at least 12 h at room temperature, pelleted by centrifugation and kept frozen as a suspension. The hydrated starches were thawed, immobilized in polyacrylamide gel [8] between microscope coverslips and imaged within a 4 h period to avoid drying. Air-dried starch was obtained by centrifuging hydrated granules at 5,000 g for 3 min. The pellet was resuspended in acetone (99.5% [v/v], Caledon Laboratory Chemicals) and centrifuged again as above. This step was repeated once again and the pellet was air-dried. Granules were stored at 20°C and 40% relative humidity for at least 24 h. For imaging, the air-dried granules were placed between microscope coverslips (without polyacrylamide gel). Ultra-dried starch was prepared in a glove box. Air-dried granules were placed in a vacuum chamber, subjected to 4 air evacuation and nitrogen refill cycles, and subsequently kept in the glove box under nitrogen atmosphere with 4.6 ppm water and 12.7 ppm oxygen for 48 h. For imaging, the ultra-dried granules were mounted between microscope coverslips (without polyacrylamide), sealed with silicone in the glove box, removed and immediately imaged. To reduce the size dependent effects (granule curvature, number of voxels in the granule and birefringence) on the laser polarization, granules with 10-15 µm diameters were studied.

2.2 Laser scanning microscope and data analysis

The home-built laser and microscope system was previously described [10, 11]. Briefly a Yb:KGW laser operating at 1028 nm wavelength with 14.3 MHz repetition rate and ~450 fs duration pulses delivered <2 nJ of pulse energy to the sample of a nonlinear optical microscope. For SHG polarization measurements, a reduced set of the double Stokes-Mueller analysis [12] was performed using the polarization-in, polarization-out (PIPO) technique [13]. In the laboratory Cartesian coordinate system, *XYZ*, is defined with respect to the principal propagation direction of the scanning laser, *Y*, where *XZ* is the image plane, while the local coordinate system, *xyz*, is associated with a cylindrically symmetric structure about *z*, where *y=Y*. Data representing the SHG intensity as a function of the laser polarization orientation ($\theta = \theta'-\delta$) and the analyzer orientation ($\phi = \phi'-\delta$) (located before the detector) was fitted using [1]:

$$I_{2\omega} = A\left(R'_{SHG} \cos\phi \cos^2\theta + \sin\phi \sin 2\theta + \cos\phi \sin^2\theta \right)^2 , \qquad (1)$$

where *A* is a fitting parameter used for normalization, δ is the angle from the laboratory *Z* axis to the crystal cylindrical axis and $R'_{SHG} = \chi^{(2)}_{zzz}/\chi^{(2)}_{zxx}$ is the second-order nonlinear optical susceptibility tensor component ratio in the local coordinate system. Fitting of PIPO SHG data for each pixel in the image was performed with custom software in MATLAB (The Mathworks, Inc.), resulting in R'_{SHG} and δ' fitting parameters. Only pixels with goodness of fit parameter $R^2>0.78$ were analyzed, and distinct granules were manually traced to find the average $R'_{SHG.}$

3. Results

3.1 SHG intensity dependency on chemical composition and hydration of starch granules

The structural origin of SHG in starch granules from WX, WT and AO barley lines was investigated at 3 hydration conditions: hydrated, air-dried, and ultra-dried. Typical images (Fig. 1) and average intensities of ≥20 granules (Table 1) show a dependency on the chemical composition and degree of hydration. The highest SHG intensity is observed in WX followed by WT granules in line with Zhuo et al. (2010) who observed this in dry rice starch [7]. The novel observation is that AO which has a more linear molecular structure also produces SHG, albeit at lower intensity than WX or WT.
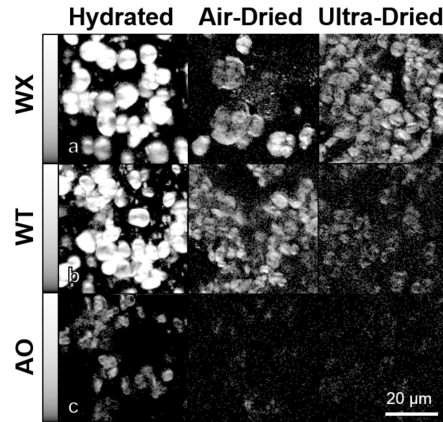

Fig. 1. SHG images of (a) WX, (b) WT, and (c) AO barley reserve starch granules at three conditions: hydrated, air-dried, and ultra-dried. Vertical linear polarized light was used for images shown with identical logarithmic intensity scales.

Table 1. The SHG intensity and R'_{SHG} of WX, WT and AO starch granules from barley studied under hydrated, air-dried and ultra-dried conditions. Values stated are granule-by-granule averages ± standard error.

Starch Type	WX	WT	AO	WX	WT	AO	WX	WT	AO
Moisture	Hydrated			Air-Dried			Ultra-Dried		
SHG Intensity	610	350	30	220	170	10	90	18	4
	± 20	± 10	± 5	± 10	± 10	± 3	± 5	± 4	± 1
Average R'_{SHG}	3.6	4.0	3.1	4.4	4.1	3.5	3.5	3.8	3.1
	± 0.1	± 0.1	± 0.1	± 0.2	± 0.1	± 0.1	± 0.1	± 0.1	± 0.1
Width R'_{SHG}	1.8	2.4	1.3	3.1	3.6	2.8	2.3	3.0	1.1
	± 0.2	± 0.1	± 0.2	± 0.1	± 0.2	± 0.4	± 0.2	± 0.2	± 0.2

An SHG intensity dependence on the hydration conditions was observed in all three starches (ANOVA p<0.01) after correcting for index mismatch between mounting hydrated granules in acrylamide vs. dry granules in air (≤30% [8]). In our previous study [8], *ab initio* calculations of R'_{SHG} of the A- and B-type crystal allomorphs revealed hydrogen and hydroxyl bonds structurally ordered in the crystalline matrix are the dominant SHG emitters. The hydration dependency shows that water is an integral part of starch granules, facilitating long-range order of the hydrogen bond network and also ordering of hydroxyl bonds. Therefore, SHG intensity of starch granules indicates that WX provides a matrix for a highly ordered crystalline structure, while AO supports a much lower crystallinity. The SHG intensity in starch granules scales with hydration level and includes weighted contributions of the constituents of the granules. More information about the structural organization of the crystalline material can be obtained using polarization-dependent SHG microscopy as discussed in the next section.

3.2 Polarization-dependent SHG studies of starch granules

The ultrastructural organization of WX, WT and AO barley starches was investigated at hydrated, air-dried and ultra-dried conditions with PIPO SHG microscopy. Typical results are shown in Fig. 2; R'_{SHG} values for each pixel are shown by color in row b and summarized with occurrence histograms in row c, while the mean and full width at half maximum (FWHM) of at least 5 granules at each condition is presented in Table 1, rows 2-3.

Overall, the differences in starch line affected the R'_{SHG} (ANOVA p<0.01). For hydrated WX and WT, the R'_{SHG} distributions are not significantly different (*t*-test p = 0.02) (Fig. 2(b1), 2(c1), 2(b2), 2(c2)), where R'_{SHG} ranges from ~2 near the starch hilum to ~5 at the periphery, but the R'_{SHG} distribution for WT has a larger shoulder towards lower values. The R'_{SHG} distribution for AO is shifted to significantly lower values (*t*-test p<0.01) (Fig. 2(b3), 2(c3)) and increases from ~2 at the starch hilum to ~4 at the periphery. Qualitatively, the R'_{SHG} distribution in WT can be understood as having a dominant contribution from amylopectin-containing structures (similar to WX), and a small contribution from more linear constituents (similar to AO) that increases the occurrence values at the shoulder of the R'_{SHG} distribution (~2.5 to ~3.5). A fit of the WT occurrence histogram by a scaled sum of WX and AO histograms (data was smoothed) revealed goodness of fit parameter $R^2 = 0.98$, and fit parameters indicated relative contributions: 31% from AO and 69% from WX, in agreement with the amylose and amylopectin content literature value in WT.
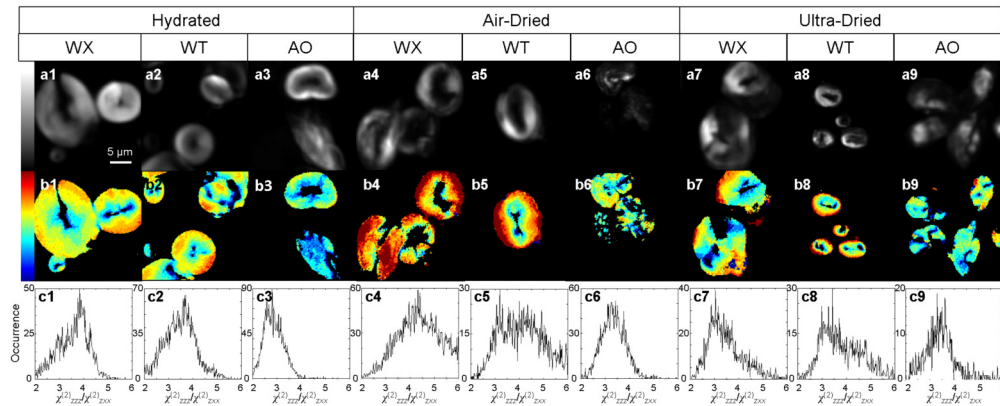

Fig. 2. SHG intensity images obtained at 81 combinations of analyzer and polarizer angles added together (a1-a9) of WX (columns 1, 4, 7), WT (columns 2, 5, 8) and AO (columns 3, 6, 9) barley starch granules studied under three conditions: hydrated (columns 1-3), air-dried (columns 4-6), and ultra-dried with nitrogen gas (columns 7-9). Fitted R'_{SHG} values for each pixel in panels a1-a9 are represented with color in panels b1-b9, where blue to red depicts R'_{SHG} values of 2 - 6. The R'_{SHG} value occurrence histograms of the fitted pixels in panels b1-b9 are shown in panels c1-c9.

An increase in R'_{SHG} occurs at the periphery of air-dried granules compared to hydrated and ultra-dried (Fig. 2). According to Eq. (A9) in [1], shifts of measured R'_{SHG} values towards 3 indicate increased orientational distribution (or disorder) of emitters, therefore indicating the orientation distribution of nonlinear dipoles around the cylindrical axis in a voxel is narrower. These larger R'_{SHG} values near the periphery of granules induce wider R'_{SHG} occurrence histograms in air-dried compared to hydrated and ultra-dried granules (Table 1). The R'_{SHG} occurrence histogram for WT starch granules has a double peak distribution (Fig. 2(c5)), and again can be understood as a weighted contribution from amylopectin (Fig. 2(c4) peak at ~4.5) and amylose (Fig. 2(c6) peak at ~3.3) containing structures. A fit of the typical WT R'_{SHG} distribution from Fig. 2 ($R^2 = 0.95$) shows 44% AO and 66% WT distribution content, which is slightly higher than the literature value of WT amylose content (~30%), implying that dehydration affects the R'_{SHG} of linear and branched polymers differently.

In the ultra-dried case, the R'_{SHG} occurrence distribution peaks at ~3 for WX and WT starches (Fig. 2(c7), 2(c8)), showing that dipoles have a large orientation distribution [1]. Severe drying of starch granules removes structural and co-crystallized water within the crystalline lamella of starch granules, reducing the crystallinity of single (Vh-type) and double (A-, and B-type) helical content of the amylopectin and amylose crystallites [14]. The R'_{SHG} distribution for ultra-dried WT cannot be explained as a weighted contribution from clustered branched and mainly linear structures, since a fit of the histogram of Fig. 2 for WT with histograms of WX and AO was unsuccessful. Larger R'_{SHG} values in the WT are less strongly affected by ultra-drying than the individual branched or linear polymer crystals in WX and AO starch lines. The ultra- and air-dried AO granules have R'_{SHG} values which are not significantly different, (p = 0.03 for an average of 5 granules), and peaking at ~3.3 (Fig. 2(c6) and 2(c9)), revealing linear polymer crystals are less variable during ultra-drying than branched polymers.

4. Discussion

The results of SHG intensity and R'_{SHG} of WX, WT and AO granules have to be compared for the same hydration condition. The wild-type amylopectin crystal contains long-range order, and facilitates the generation of SHG much more efficiently (~20 times) than amylose containing structures, indicating that amylose forms aggregates with much lower crystalline order. This interpretation is in line with the results showing that AO have R'_{SHG} values distributed around 3, while for WT and WX granules the R'_{SHG} values reach higher than 4 (Fig. 2). The $R'_{SHG} = 3$ when orientation of the nonlinear dipole reaches 39.2° from the cylindrical axis, and smaller R'_{SHG} indicate even larger deviations of the orientation angles, while larger R'_{SHG} show that the nonlinear dipole orientations are getting progressively closer to the cylindrical axis.

Hydration strongly affects all three starch lines. The higher SHG intensity in hydrated granules occurs due to more ordered hydroxide and hydrogen bonds within crystallites, and the resulting increased long-range order reduces the R'_{SHG} width, in agreement with the small angle X-ray and neutron data supported liquid crystal model of starch, which shows increased long-range ordering in the smectic (hydrated) phase of starches [15]. The distribution of R'_{SHG} in air-dried barley starch granules is wider and has a higher maximum value, while in hydrated granules it is narrow with lower maximum R'_{SHG}. The R'_{SHG} distribution shows heterogeneity of the structure within the granule which ranges from lower values near the hilum to higher values near the periphery. Hydrated granules are more homogeneous compared to the air-dried granules. Their lower R'_{SHG} values (4 to 5) show that structural and co-crystalized water has a relatively broad orientation distribution in hydrated granules, while the higher R'_{SHG} values in air-dried granules are attributed to co-crystallized water that remains after drying and has a hydroxide and hydrogen bond network oriented closer to the crystalline axes.

The reduced R'_{SHG} in ultra-dried granules likely occurs due to the same phenomenon as the R'_{SHG} value near a starch hilum. A voxel near the hilum contains polymer crystals with a wide distribution of orientations, while a voxel far away from the hilum contains a much more narrow distribution, resulting in reduced R'_{SHG} towards an expected value of 3 near the hilum [4].

5. Conclusions

SHG intensity in starches is affected by endogenous (genetic) and external factors, such as hydration, and is correlated with crystallinity measurements previously observed by powder X-ray diffraction. Since SHG can visualize individual granule regions quickly without extensive sample preparation, it is a very convenient technique and should be compared to other starch crystallinity measurements including NMR, X-ray, electron and neutron diffraction, polarized light microscopy as well as hydrolysis. SHG intensity variation in WX,

WT and AO starches at different hydration indicates that amylopectin crystallites contain highly ordered structural and co-crystallized water, while polymers with reduced branching similar to amylose still crystallize, although to a lower extent than WT or WX lines, and retain preferentially oriented hydroxide and hydrogen bonds. Therefore it is likely that wild-type amylose also behaves similarly. R'_{SHG} shows structural heterogeneity of the granule spanning from the hilum to the periphery. At high moisture conditions both structural and co-crystallized water results in lower R'_{SHG} indicating broader orientation distribution of nonlinear dipoles. Removal of structural water at moderate moisture conditions leads to remaining co-crystalized water oriented closer to the axis of various glucan helices, while ultra-dry conditions increase the structural disorder. Therefore, R'_{SHG} represents a highly-sensitive measurement of ultrastructure in starch.

Acknowledgments